The anomaly Cu doping effects on LiFeAs superconductors

OPEN ACCESS
IOP Publishing
Journal of Physics: Condensed Matter
J. Phys.: Condens. Matter **26** (2014) 435703 (6pp)
doi:10.1088/0953-8984/26/43/435703

The anomaly Cu doping effects on LiFeAs superconductors

L Y Xing, H Miao, X C Wang, J Ma, Q Q Liu, Z Deng, H Ding and C Q Jin

Beijing National Laboratory for Condensed Matter Physics, Institute of Physics, Chinese Academy of Sciences, Beijing 100190, People's Republic of China

E-mail: wangxiancheng@iphy.ac.cn and Jin@iphy.ac.cn

Received 1 May 2014, revised 6 August 2014
Accepted for publication 22 August 2014
Published 9 October 2014

Abstract

The Cu substitution effect on the superconductivity of LiFeAs has been studied in comparison with Co/Ni substitution. It is found that the shrinking rate of the lattice parameter c for Cu substitution is much smaller than that of Co/Ni substitution. This is in conjugation with the observation of ARPES that shows almost the same electron and hole Fermi surfaces (FSs) size for undoped and Cu substituted LiFeAs sample, except for a very small hole band sinking below Fermi level with doping. This indicates that there is little doping effect at Fermi surface by Cu substitution, in sharp contrast to the more effective carrier doping effect by Ni or Co.

Keywords: iron based superconductor, '1 1 1' type, anomaly doping effects

(Some figures may appear in colour only in the online journal)

1. Introduction

Since the discovery of La[$O_{1-x}F_x$]FeAs in 2008 [1], various classes of iron-based superconductors, such as '122' [2] '111' [3] or '11' [4], are reported [5–7]. These iron based superconductors contain superconducting [FePn(Se)] (where Pn is pnictide element of As or P) layers which are interlaced by charge carrier reservoir layers. Most of their parent compounds are in the form of antiferromagnetic spin density wave (SDW) states. The antiferromagnetism can be suppressed by either introducing charge carrier or applying pressure, leading to superconductivity. Superconductivity can be induced by various methods of element substitution, either in the plane of [FePn(Se)] layer, or out of the plane. For instance, in the case of $BaFe_2As_2$, K-substitution at the Ba site, Co or Ni substitution at the Fe site, or P substitution at the As site, will induce superconductivity respectively [2, 8–10]. The partial replacement of Ba^{2+} ion by K^+ ion will introduce hole-like charge carrier to the system, while chemical pressure is applied when As atoms are substituted partially by P atoms. However, the effect of substitution at Fe site is quite different [11–21]. It seems that both Co or Ni substitution at Fe site introduce itinerant electrons, as experimentally indicated by ARPES [15–17] and transport measurements [16–20], or x-ray emission spectroscopy measurements [21, 22]. On the other hand, the density-functional studies of the $Fe_{1-x}Cu_xSe$ show that, although Cu serves as an effective electron dopant, it is still a source of strong scattering [23]. Recently, the ARPES studies of $Ba(Fe_{1-x}Cu_x)_2As_2$ [24] and the work on $NaFe_{1-x}Cu_xAs$ [25] have revealed that part of electrons doped by substitution of Cu are almost localized.

To date, the research on this issue is mainly limited to the Ba-122 system, since it is relative easy to grow high quality single crystals. In fact, '1 1 1' type iron based superconductors are unique. In the structure of '1 1 1' type compounds, the [FePn] layers are intercalated with two layers of alkali metals atoms [3, 26]. The '1 1 1' system shows systematic evolution of superconductivity as a function of Co/Ni doping [27] or pressure [28–30]. The crystal can be easily cleaved and results in equivalent and neutral counterparts with identical surface versus bulk electronic structures, which is favored by ARPES [31–33]. Moreover, it can be referred as an electron over doped superconductor [34, 35]. When doped with Co/Ni in the parent LiFeAs, it presents no SDW transition and no dome like superconducting phase diagram, but a linear suppression of T_c [27], making this compound a good candidate for studying the effect of TM substitution. So far, the reported chemical doping effect of LiFeAs is limited to Co/Ni substitution [27, 33]. In this work, we study the effect of Cu substitution in comparison with Co/Ni substitution on the superconductivity of single

crystals in LiFeAs system. We found that the behaviour of Cu substitution is quite different from that of Co/Ni substitution in that most of the 3 d electrons from Cu dopant are mostly localized.

2. Experimental details

Single crystals of $LiFe_{1-x}TM_xAs$(TM = Cu, Co/Ni) were grown by self-flux method, using Li_3As, As and $Fe_{1-x}TM_xAs$ powder as the starting materials. The precursor Li_3As was obtained by mixing Li lump and As powder, which was then sealed in an evacuated titanium tube and sintered at 650 °C for 10 h. $Fe_{1-x}TM_xAs$ were prepared by mixing Fe, Cu (or Co/Ni) and As powder thoroughly, pressed into pellets, sealed in a evacuated quartz tube and sintered at 700 °C for 30 h. To ensure the homogeneity of the product, these pellets were grounded and heated again. The stoichiometric amount of Li_3As, $Fe_{1-x}TM_xAs$ and As powder were weighed according to the element ratio of $Li(Fe_{1-x}TM_x)_{0.3}As$. The mixture was grounded and put into alumina crucible and sealed in Nb crucible under 1 atm of Argon gas. The Nb crucible was then sealed in the evacuated quartz tube, heated to 1100 °C and slowly cooled down to 700 °C at a rate of 3 °C hr^{-1} to grow single crystals. The obtained $LiFe_{1-x}TM_xAs$ single crystals have the typical size of $10\times6\times0.5$ mm, as shown in figure 1(*a*). All sample preparations, except for sealing, were carried out in the glove box filled with high purity Argon gas.

The element composition of the $LiFe_{1-x}TM_xAs$ single crystals was checked by energy dispersive x-ray spectroscopy (EDS). These single crystals were characterized by x-ray diffraction. The transport measurements were carried on commercial physical properties measurement system (PPMS) using the four probe method. The dc magnetic susceptibility was measured with a magnetic field of 30 Oe using a superconducting quantum interference device (SQUID). ARPES studies were performed at beam lines PGM and Apple-PGM of the Synchrotron Radiation Center, Wisconsin, equipped with Scienta R4000 analyzer and SES 200 analyzer, respectively. The energy and angular resolutions of the ARPES measurements were set at 20–25 meV and 0.2°, respectively. The samples were cleaved *in situ* and measured at 30 K under a vacuum of 5×10^{-11} torr. The incident photon energy was chosen to be $h\nu = 51$ eV.

3. Results and discussions

The element composition checked by EDS is close to the nominal one. Thus, here the nominal concentration is used in the sample chemical formula. The typical x-ray diffraction pattern of the *0 0 l* reflections for $LiFe_{1-x}TM_xAs$ single crystal is shown in figure 1(*a*). From the diffraction pattern, the lattice constant *c* was calculated and the obtained c-axis values were plotted as a function of doping level *x* for Cu, Co/Ni substituted samples (as shown in figure 1(*b*)), indicating a successful chemical substitution. However, in the case of Cu substituted samples, the lattice constant *c* shrinks by ~0.06% at the doping level $x = 0.06$; while for the Co/Ni substituted samples at the same doping level, the *c* value decreases by ~0.3%, which is much larger than that of Cu substituted samples. This will be further discussed in conjugation with ARPES measurements.

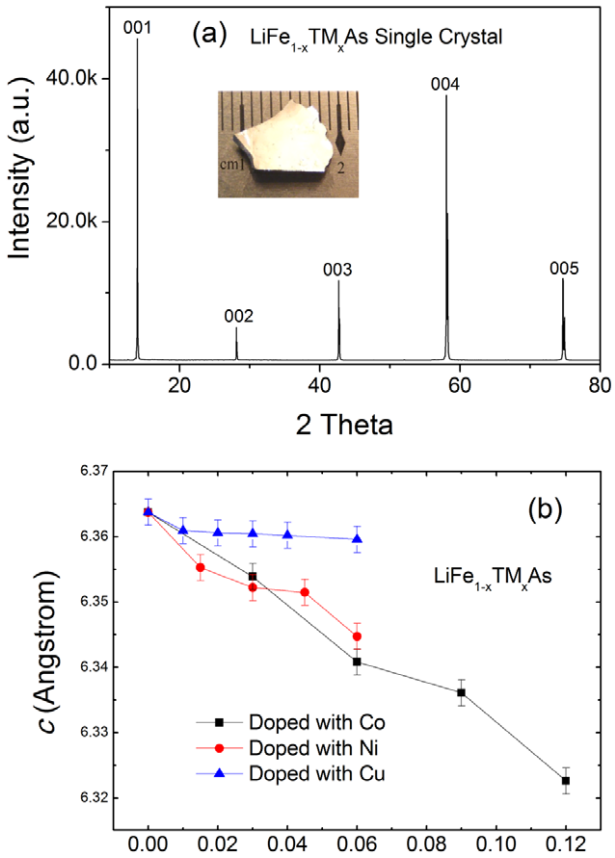

Figure 1. (*a*) The typical XRD patterns for $LiFe_{1-x}TM_xAs$ single crystals. The inset is the photo of LiFeAs single crystal with typical size of 10 × 6 × 0.5 mm; (*b*) the dependence of lattice constant c on doping level *x* for $LiFe_{1-x}Tm_xAs$ single crystal (Tm = Co, Ni and Cu).

Figure 2 presents the transport and magnetic data of Cu substituted LiFeAs single crystals. The temperature dependence of in-plane resistivity ρ is shown in figure 2(*a*) and the magnetic susceptibility in both zero field cooling (ZFC) and field cooling (FC) modes are shown in figure 2(*b*). For undoped LiFeAs crystal, the resistivity drops sharply to zero at ~17 K with a narrow superconducting transition width ΔT ~1.1 K and the residual resistivity ration (RRR), defined as the ratio of the resistivity at 300 K and residual resistivity ρ_0, which is determined by extending from the range right above T_c found to be 60. Upon Cu doping, the effect of its scattering on electron mobility increases and leads to the increase of resistivity (as shown in figure 2(*a*)), implying the localization of doping carriers from Cu that acts more like an impurity center. The magnetic susceptibility of LiFeAs crystal shown in figure 2(*b*) suggests bulk superconductivity with $T_c \sim 16$ K, which is defined by the bifurcation point between ZFC and FC magnetic susceptibility as consistent with transport data. As shown in figure 2(*a*) and figure 2(*b*), the T_c of $Li(Fe_{1-x}Cu_x)As$ is gradually suppressed, reaching to ~3 K at the Cu doping level of 7%. The T_c extracted from the resistivity and magnetic measurements as a function of doping level are plotted in figure 2(*c*), showing an almost linear dependence on Cu doping level. The red line represents a linear fitting to T_c change as

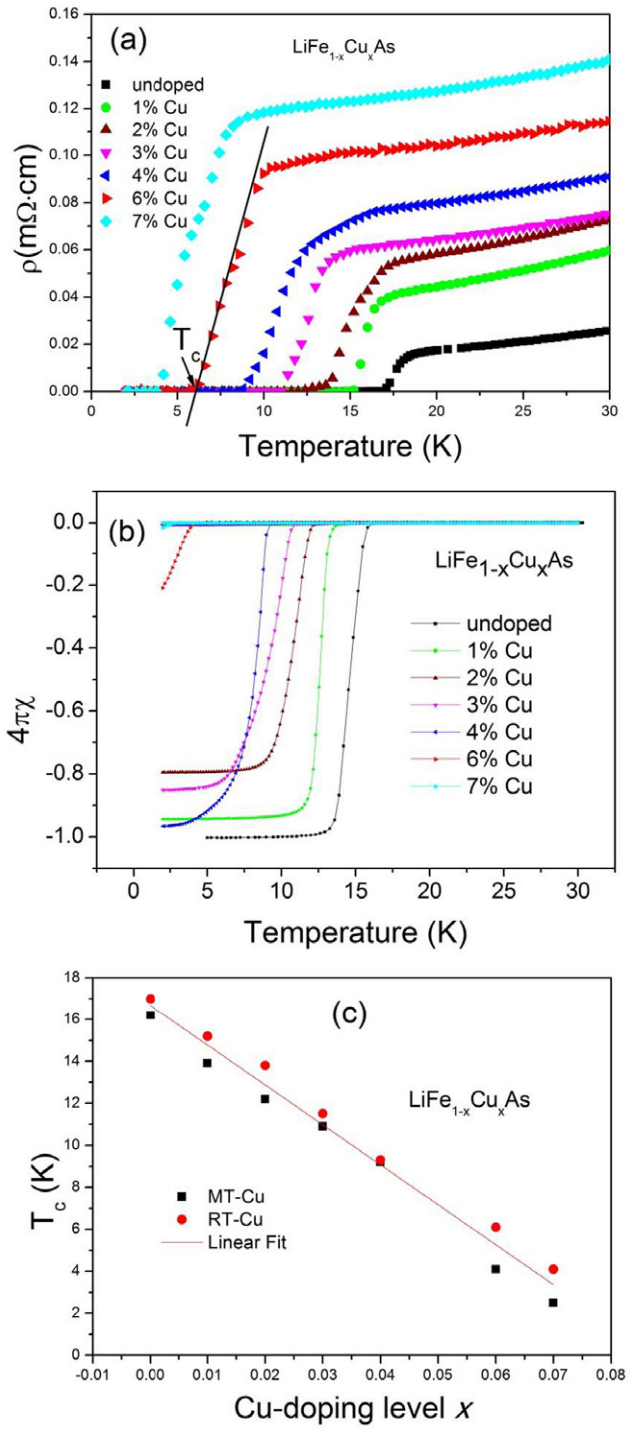

Figure 2. (*a*) The temperature dependence of resistivity for $LiFe_{1-x}Cu_xAs$ single crystal. (*b*) The magnetic susceptibility of $LiFe_{1-x}Cu_xAs$ single crystal. (*c*) The critical temperature plotted as a function of Cu-doped level x. The red line is the linear fit of T_c versus Cu-doped level x for both the magnetic susceptibility measurement data and resistance measurement data.

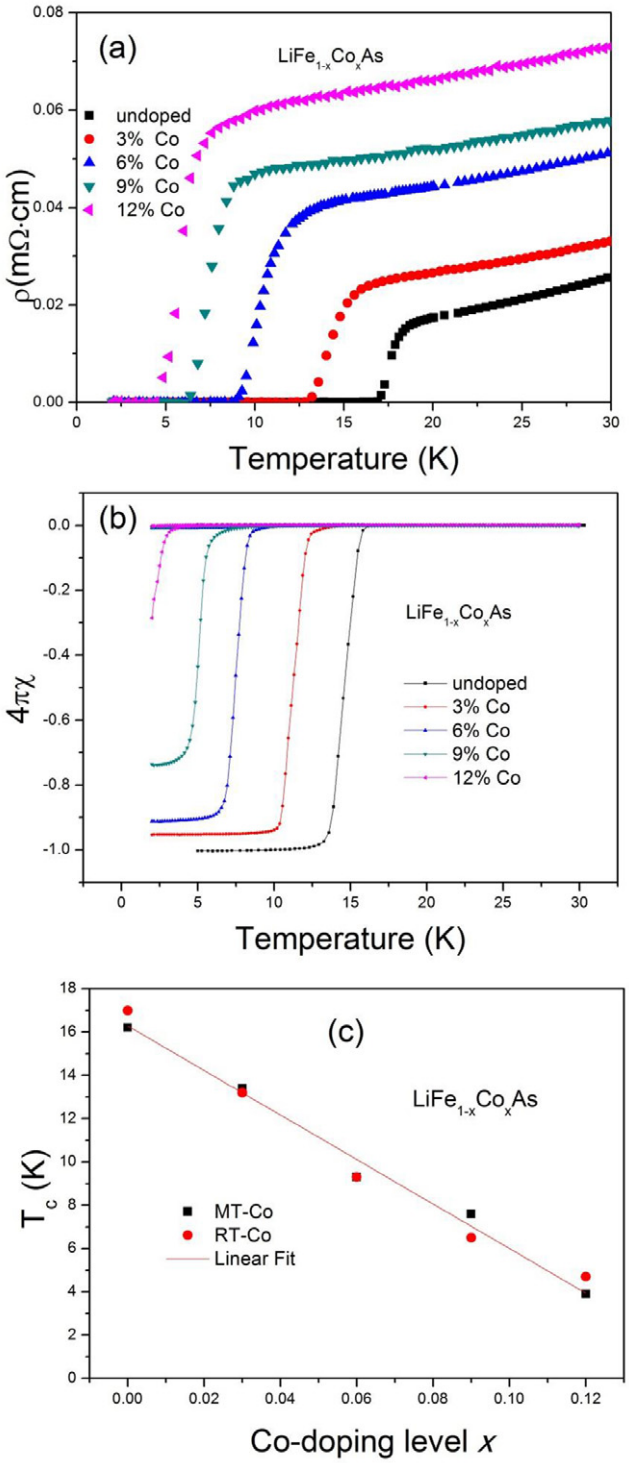

Figure 3. (*a*) The temperature dependence of resistivity for $LiFe_{1-x}Co_xAs$ single crystal. (*b*) The magnetic susceptibility of $LiFe_{1-x}Co_xAs$ single crystal. (*c*) The critical temperature plotted as a function of Co-doped level x. The red line is the linear fit of T_c versus Co-doped level x for both the magnetic susceptibility measurement data and resistance measurement data.

function doping level, which demonstrates T_c decreases at a rate about 1.9 K per 1% Cu dopant in $Li(Fe_{1-x}Cu_x)As$.

For Co substituted LiFeAs single crystal samples, the ρ-T curve and magnetic susceptibility measurements are shown in figures 3(*a*) and 3(*b*), respectively. All the samples show a sharp superconducting transition. The T_c decreases with increasing Co doping level and is suppressed down to ~4 K by 12% Co doping. Figure 3(*c*) presents the linear fitting result for the data of T_c versus Co doping level, showing an approximately 1 K suppression rate per 1% Co doping.

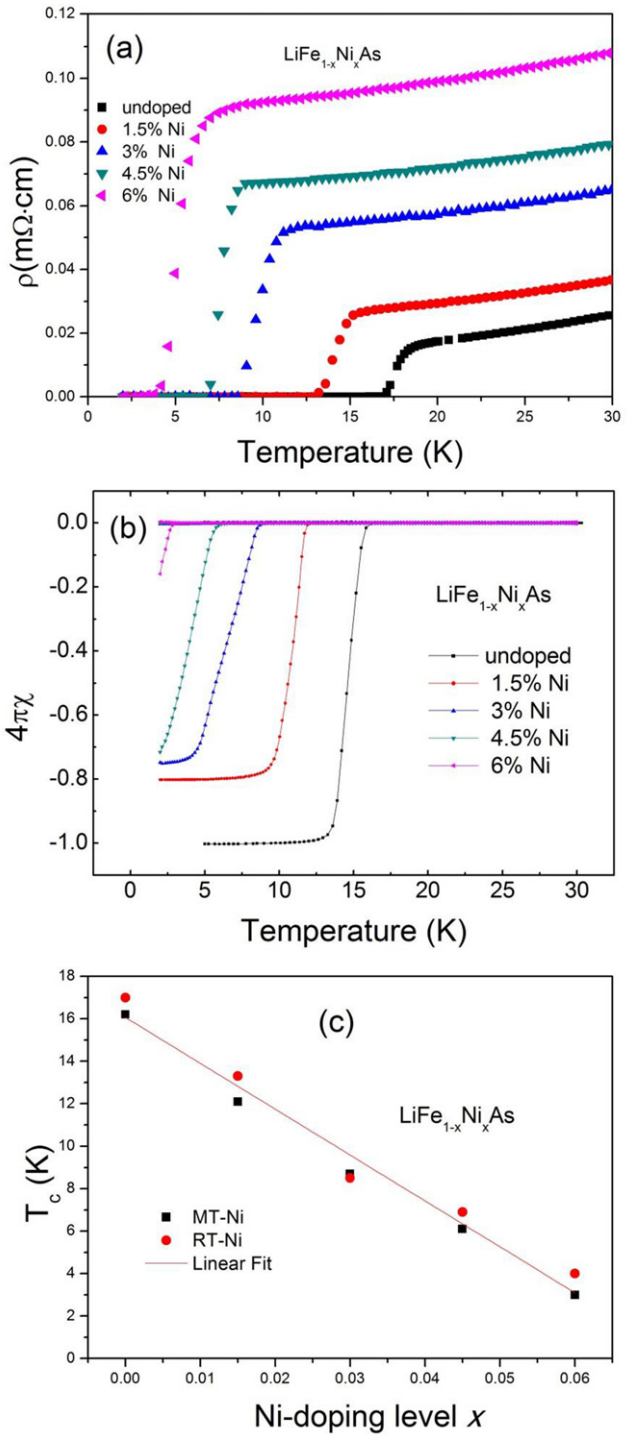

Figure 4. (*a*) The temperature dependence of resistivity for $LiFe_{1-x}Ni_xAs$ single crystal. (*b*) The magnetic susceptibility of $LiFe_{1-x}Ni_xAs$ single crystal. (*c*) The critical temperature plotted as a function of Ni-doped level x. The red line is the linear fit of T_c versus Ni-doped level x for both the magnetic susceptibility measurement data and resistance measurement data.

Figures 4(*a*) and 4(*b*) are the transport and magnetic properties for $LiFe_{1-x}Ni_xAs$ crystals respectively, while the T_c value versus Ni-doping level is plotted and fitted linearly as shown in figure 4(*c*). T_c is linearly suppressed by Ni doping with a rate of about 2.2 K per 1% Ni doping.

We found that the suppression rate of T_c for Ni substitution is twice that of Co substitution, implying that Co and Ni substitution introduce one and two more itinerant electrons respectively, which is consistent with the change of lattice parameter. Similar behavior had been observed in Co and Ni doped Ba 122 system [36].

To further verify the localization tendency of Cu doped electron, which is different with the Co/Ni substitution with less change of lattice parameter for Cu doping (as shown in figure 1(*b*)), we measured the electronic structure by using APRES technique in order to get a straightforward electronic structure picture of Cu doped LiFeAs. It has been experimentally [31] proven that the surface of LiFeAs preserves its bulk properties. Therefore ARPES reflects the intrinsic properties for the LiFeAs crystals. Previously ARPES were used to study the Fermi surface evaluation when Fe is partially substituted by Co [33]. The results show that Co substitution introduces electron type charge carriers and results in chemical potential shifting upwards, indicating electron doping. The Fermi surface (FS) mappings along the Γ–M high symmetry line from ARPES for undoped and Cu 6% doped LiFeAs are shown in figures 5(*a*) and 5(*b*), respectively. To check how FSs change with Cu substitution, extracted k_F locus were plotted in figures 5(*a*), 5(*b*) and 5(*e*), respectively. Red circles and green triangles represent undoped and Cu 6% doped $Li(Fe_{1-x}Cu_x)As$, respectively. The results reveal no significant difference in these two different crystals, except for the small hole FS observed in LiFeAs, which disappeared in the Cu 6% doped $Li(Fe_{1-x}Cu_x)As$, indicating small electron doping effect. Additionally, the normal state (T = 30 K) high resolution ARPES intensity plots along the Γ–M high symmetry line are shown in figures 5(*c*) and 5(*d*), respectively. The incident light was set to 51 eV ($k_z = 0$) with its polarization perpendicular to the mirror plane to select odd symmetry orbitals. Red and green solid circles were used to extract the band dispersion, which generates the small hole FS in LiFeAs. It is clear that the extracted band crosses E_F in LiFeAs but sinks below E_F in Cu 6% sample. Our results show that, unlike Co and Ni substituted LiFeAs [33], where extra electrons cause Fermi level to shift, the FSs of Cu substituted LiFeAs remained almost intact. Hence, the 3 d electrons from Cu dopant in LiFeAs are more localized and contribute little to the FSs. Berlijn *et al* studied disorder effects of Co and Zn substitution in Ba122 system [37]. They found that the calculated Femi surface behaviors of Zn substitution induced deep impurity level that is quite different from the effect of Co doping. Recently Ideta *et al* reported strong localization effects in Zn substituted $BaFe_2As_2$, wherein all the extra electrons are localized at the state of ∼10 eV below FSs and do not contribute to the chemical potential shift at all [38]. Our results can be explained from the d-band partial density of states of Co, Ni and Cu in iron based superconductors. The behavior of Co or Ni substitution follows a rigid band model due to the fact that the d-bands of Co and Ni overlap with Fe d-band and are featureless compared with Fe d-band; whereas Cu presents deeper impurity potential of ∼4 eV [22], which localizes most of the Cu 3 d orbital electrons. This is consistent with the lesser contraction of lattice parameters

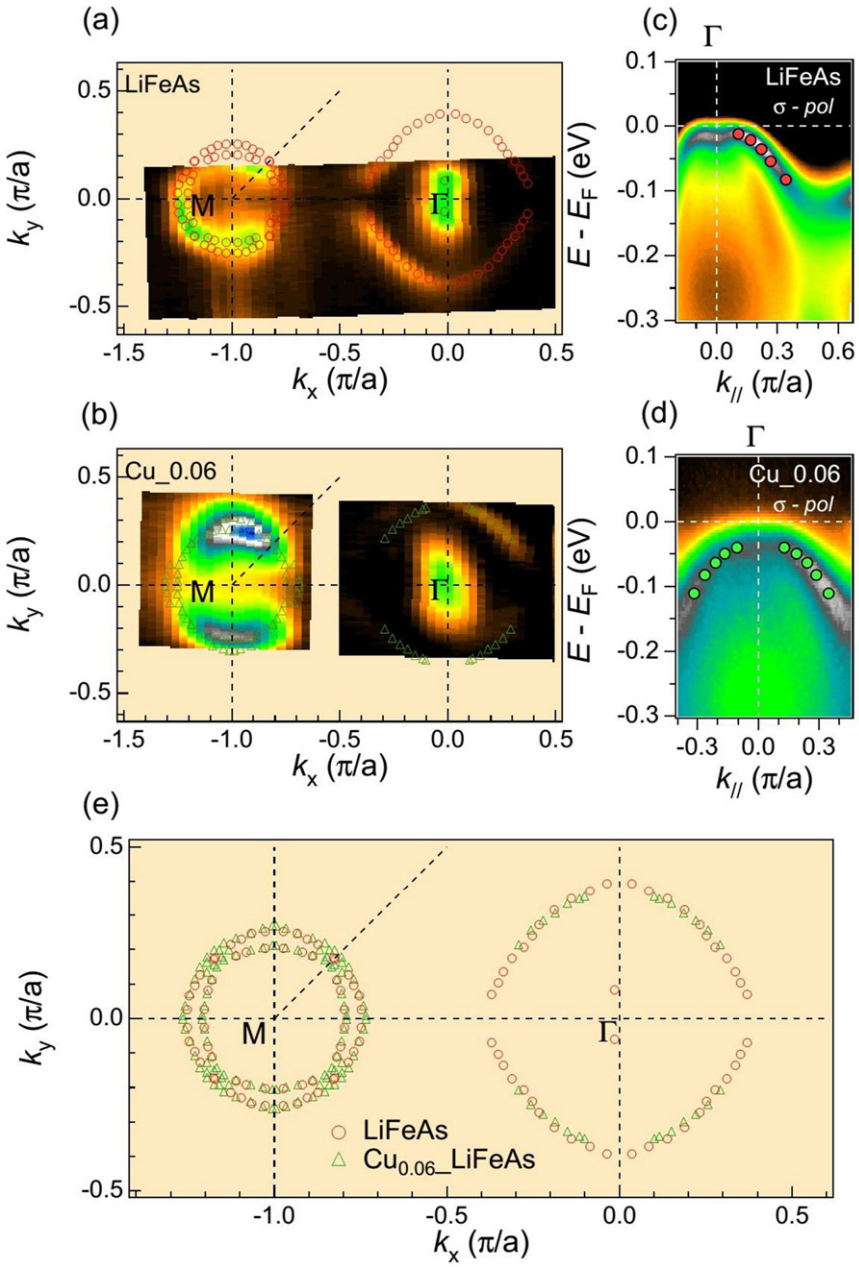

Figure 5. (*a*), (*b*) ARPES intensity at E_F of LiFeAs and Cu 6% doped LiFeAs with photon energy at 51 eV. The intensity is obtained by integrating the spectra within ± 10 meV with respect to E_F. (*c*), (*d*) ARPES high resolution cut along high symmetry line Γ–M at $k_z = 0$. (*e*) Extracted k_F locus of LiFeAs and Cu 6% doped LiFeAs.

by Cu substitution compared with Co/Ni substitution, where in itinerant electrons are induced. Although there is a small electron doping effect by Cu substitution in LiFeAs system, the doped coherent electrons would be even smaller considering the effect of disorder with strong impurity potential [38]. Hence, the suppression of T_c by Cu substitution is mainly from strong impurity scattering instead of carrier density change. Here we found that Cu doping results in the sinking of the small hole band below E_F in $LiFe_{0.94}Cu_{0.06}As$ which contributes to approximately only 1% mobile electron carriers(normalized to 0.17 electron / Cu doping). Therefore, the Cu doping is more localized in LiFeAs system and quantitatively different from Cu doped other systems [23–25]. For example, the practical doped mobile carriers in $Ba(Fe_{1-x}Cu_x)_2As_2$ [24] are about 1 electron per Cu as calculated from the change of the Fermi Surface volume, which is much higher than 0.17 electron per Cu in our LiFeAs system.

On the other hand, it is interesting to compare Cu doping with Ru doping. Since Ru is isovalent to Fe (within the same column in periodic table), Ru doping will not introduce carriers theoretically. The experiments of ARPES verified that Ru is isoelectronic substitution [39]. Therefore, Cu doping versus Ru doping represent two typical cases that do not introduce carriers. However, the mechanism is different, as for Cu doping case the 'carriers' are localized, while for Ru doping there is no additional carriers induced.

In summary, series of $LiFe_{1-x}Cu_xAs$ single crystals were grown by self-flux method. Based on systematic

investigations of superconducting transitions, crystal versus electronic structure evolution with Cu doping level, we found that behaviors of Cu substitution are different from those of Co/Ni substitution in both change rates of Tc, as well as lattice parameters as function of doping level. ARPES measurements indicated that most of the 3 d valence electrons from Cu dopant are localized, resulting in almost intact Fermi surfaces for Cu doped LiFeAs except for a very small hole band sinking below Fermi level, which is also quite different from the doping effects in other systems.

Acknowledgments

The work is supported by NSF and MOST of China through research projects. We are grateful to PGM and Apple PGM of the Synchrotron Radiation Center Wisconsin for supporting ARPES experiments.

References

[1] Kamihara Y, Watanabe T, Hirano M and Hosono H 2008 *J. Am. Chem. Soc.* **130** 3296
[2] Rotter M, Tegel M and Johrendt D 2008 *Phys. Rev. Lett.* **101** 107006
[3] Wang X C, Liu Q Q, Lv Y X, Gao W B, Yang L X, Yu R C, Li F Y and Jin C Q 2008 *Solid State Commun.* **148** 538
[4] Hsu F C *et al* 2008 *Natl Acad. Sci. USA* **105** 14262
[5] Ishida K, Nakai Y and Hosono H 2009 *J. Phys. Soc. Japan* **78** 062001
[6] Stewart G 2011 *Rev. Mod. Phys.* **83** 1589
[7] Wang F and Lee D H 2011 *Science* **332** 200
[8] Sefat A S, Jin R Y, McGuire M A, Sales B C, Singh D J and Mandrus D 2008 *Phys. Rev. Lett.* **101** 117004
[9] Li L J *et al* 2009 *New. J. Phys.* **11** 025008
[10] Jiang S, Xing H, Xuan G, Wang C, Ren Z, Feng C, Dai J, Xu Za and Cao G 2009 *J. Phys.: Condens. Matter* **21** 382203
[11] Wadati H, Elfimov I and Sawatzky G A 2010 *Phys. Rev. Lett.* **105** 157004
[12] Bittar E M, Adriano C, Garitezi T M, Rosa P F S, Mendonca-Ferreira L, Garcia F, Azevedo G d M, Pagliuso P G and Granado E 2011 *Phys. Rev. Lett.* **107** 267402
[13] Nakamura K, Arita R and Ikeda H 2011 *Phys. Rev.* B **83** 144512
[14] Konbu S, Nakamura K, Ikeda H and Arita R 2012 *Solid State Commun.* **152** 728
[15] Sekiba Y *et al* 2009 *New J. Phys.* **11** 025020
[16] Liu C *et al* 2010 *Nat. Phys.* **6** 419
[17] Neupane M *et al* 2011 *Phys. Rev.* B **83** 094522
[18] Fang L, Luo HQ, Cheng P, Wang Z S, Jia Y, Mu G, Shen B, Mazin I I, Shan L, Ren C and Wen H H 2009 *Phys. Rev.* B **80** 140508
[19] Rullier-Albenque F, Colson D, Forget A and Alloul H 2009 *Phys. Rev. Lett.* **103** 057001
[20] Canfield P C, Bud'ko S L, Ni N, Yan J Q and Kracher A 2009 *Phys. Rev.* B **80** 060501
[21] McLeod J A *et al* 2012 *J. Phys.:Condens. Matter* **24** 215501
[22] Kim M G *et al* 2012 *Phys. Rev. Lett.* **109** 167003
[23] Chadov S, Schärf D, Fecher G H, Felser C, Zhang L and Singh D J 2010 *Phys. Rev.* B **81** 104523
[24] Ideta S *et al* 2013 *Phys. Rev. Lett.* **110** 107007
[25] Cui S, Kong S, Ju S, Wu P, Wang A, Luo X, Chen X, Zhang G and Sun Z 2013 *Phys. Rev.* B **88** 245112
[26] Deng Z, Wang X C, Liu Q Q, Zhang S J, Lv Y X, Zhu J L, Yu R C and Jin C Q 2009 *EPL Europhys. Lett.* **87** 37004
[27] Pitcher M J *et al* 2010 *J. Am. Chem. Soc.* **132** 10467
[28] Zhang S J *et al* 2009 *EPL Europhys. Lett.* **88** 47008
[29] Zhang S *et al* 2009 *Phys. Rev.* B **80** 014506
[30] Gooch M, Lv B, Tapp J H, Tang Z, Lorenz B, Guloy A M and Chu P C W 2009 *EPL Europhys. Lett.* **85** 27005
[31] Borisenko S V *et al* 2010 *Phys. Rev. Lett.* **105** 067002
[32] Umezawa K 2012 *Phys. Rev. Lett.* **108** 037002
[33] Ye Z R *et al* 2013 arXiv:1303.0682v1
[34] Tapp J H, Tang Z J, Lv B, Sasmal K, Lorenz B, Chu P C W and Guloy A M 2008 *Phys. Rev.* B **78** 060505
[35] Wang M *et al* 2012 *Phys. Rev.* B **86** 144511
[36] Ni N, Thaler A, Yan J Q, Kracher A, Colombier E, Bud'ko S L and Canfield P C 2010 *Phys. Rev.* B **82** 024519
[37] Berlijn T, Lin C H, Garber W and Ku W 2012 *Phys. Rev. Lett.* **108** 207003
[38] Ideta S *et al* 2013 *Phys. Rev.* B **87** 201110
[39] Xu N *et al* 2012 *Phys. Rev.* B **86** 064505